Proceedings of the ASME 2023 42nd International Conference on Ocean, Offshore and Arctic Engineering
OMAE2023
June 11-16, 2023, Melbourne, Australia

OMAE2023-105070

WAVE ATTENUATION BY SUBMERGED OSCILLATING PLATES

Yongbo Chen
College of Shipbuilding Engineering
Harbin Engineering University
Harbin, China
Email: chenyongbo@hrbeu.edu.cn

Masoud Hayatdavoodi
Civil Engineering Department
University of Dundee
Dundee, DD1 4HN, UK
& College of Shipbuilding Engineering
Harbin Engineering University
Harbin, China
Email: mhayatdavoodi@dundee.ac.uk

Binbin Zhao
College of Shipbuilding Engineering
Harbin Engineering University
Harbin, China
Email: zhaobinbin@hrbeu.edu.cn

R. Cengiz Ertekin
Ocean and Resources Engineering Department
University of Hawaii at Manoa
Honolulu, HI 96822, USA
& College of Shipbuilding Engineering
Harbin Engineering University
Harbin, China
Email: ertekin@hawaii.edu

ABSTRACT

Submerged oscillating plates are used as heaving plates to reduce the motion of floating objects, in wave energy devices to extract the wave energy, and as breakwaters to attenuate the wave field in shallow water. In this study, we consider a horizontal, submerged plate in shallow water that is allowed to oscillate in the vertical direction due to the wave loads. The plate is attached to a linear spring and damper to control the oscillations. The focus of this study is on the transformation of the wave field by the submerged oscillating plate. To estimate the energy attenuation, wave reflection and transmission coefficients are determined from four wave gauges; two placed upwave and two placed downwave of the oscillating plate. The fluid is governed by the nonlinear Level I Green-Naghdi (GN) equations, coupled with the equations of vertical motion of the plate to determine its oscillations. Time series of water surface elevation recorded at gauges upwave and downwave of the plate, and the wave-induced plate oscillations, obtained by the GN model are compared with available laboratory experiments and other data, and very good agreement is observed. Wave reflection and transmission coefficients are then determined for a range of involved parameters, including wave condition (wave height and wave period), initial submergence depth of the plate, plate length, and the spring-damper system. It is found that a single submerged oscillating plate can have remarkable effect on the wave field, and that nonlinearity plays an important role in this wave-structure interaction problem. Discussion is provided on how the wave reflection and transmission vary with the wave condition, plate characteristic, initial submergence depth and spring-damper system.

Keywords: Submerged oscillating plates, GN equations, shallow water waves, wave reflection and transmission

INTRODUCTION

Submerged horizontal plates are applied as wave breakers to mitigate extreme wave loads on nearshore and structures. Wave scattering characteristics by submerged fixed plates have been investigated by many researchers, see e.g. [1], [2], [3], [4], [5] and [6]. Compared to submerged fixed plates, oscillating horizontal plates are more efficient to attenuate waves, illustrated by [7], [8] and [9]. Submerged horizontal plates are also applied as submerged wave energy devices. Studies performed by [10] and [11] showed that wave fields are modified due to the presence of submerged wave energy converters. Waves deformed by submerged wave energy devices of submerged horizontal plates, studied by e.g. [12] and [13], and plate arrays studied by e.g. [14] and [15], are investigated.

Submerged horizontal plates experience oscillatory wave forces when waves propagate over the plates. Therefore the horizontal plate if designed appropriately, can oscillate in the vertical direction due to the vertical wave-induced force. Wave-induced oscillations of the plate are affected by various parameters, including wave conditions, initial submergence depths of the plate, and the attached spring-damper system which is used to control plate's oscillations. At the same time, plate oscillations also alter wave field, i.e. the wave field is attenuated by oscillating plates. Hence, this is a fluid-structure-fluid problem, understanding of which requires information about the fluid domain, fluid-induced oscillations of the plate, and the effect of the plate on the fluid domain, and the coupling between these.

Many studies are conducted to understand transformation of waves propagating over a submerged fixed plate, see e.g. [16], [4] and [17]. By comparing surface elevation time series upwave and downwave of the plate, studies of [18] illustrated that waves attenuated by an oscillating plate are different compared to a fixed plate. However, studies of wave attenuation by a submerged oscillating plate are very limited.

Wave attenuation by oscillating plates were investigated numerically by [7], [8] and [9]. In work of [7], a numerical wave tank was established by using the potential theory, to investigate how waves are attenuated by a submerged oscillating horizontal plate, and wave reflection and transmission coefficients are calculated to determine the wave attenuation. In that study, critical spring stiffness values were determined to reduce the transmission coefficients to near zero. Using the smoothed particle hydrodynamics method, wave attenuation by an oscillating plate for various initial submergence depths was investigated by [8]. A more recent study by [9] considered wavelength's effect on waves attenuated by oscillating plates by use of the computational fluid dynamics method. All the studies, however, are confined to deep to intermediate wave conditions subject to very limited wave-plate cases.

Submerged oscillating horizontal plates, used for mitigation of large waves and for wave energy production applications, are placed in shallow waters. Wave transformation in shallow water by seafloor or by an object requires a proper understanding of nonlinearity, i.e. the ratio of wave height to water depth, and dispersion, the ratio of water depth to wavelength. The nonlinearity plays an important role when wave propagates over an oscillating submerged plate due to the sudden change of the water depth upwave and above the plate. Dispersion, on the other hand, causes the formation of higher oscillatory components as the wave passes over the plate towards downwave region. Thus the effect of nonlinearity and dispersion is essential to the problem of wave attenuation by submerged oscillating plates.

In this study, we use a nonlinear, dispersive approach to study attenuation of waves by a submerged, oscillating horizontal plate, namely the Level I Green-Naghdi (GN) equations. We follow similar approach recently proposed by [19] to study this problem. The wave attenuation is investigated by defining wave reflection and transmission coefficients.

The plate is allowed to oscillate only in the vertical direction and its oscillations are controlled by a linear spring and damper. A wide range of parameters are considered, including wave condition, plate length, initial submergence depth of the plate, spring stiffness and damping coefficient, to study their effect on the wave reflection and transmission.

The Level I GN theory is introduced first, followed by the equation of motion of the plates. Results of surface elevation time series are first compared with available data. This is followed by discussion on the wave attenuation by an oscillating submerged horizontal plate. Then variations of wave reflection and transmission coefficients with different variables are presented and discussed, where contributions of higher-order harmonics are also investigated. Results of oscillating plates are then compared to a fixed, horizontal plate. The concluding remarks section is followed to close the paper.

THE LEVEL I GN THEORY

The wave attenuation by a submerged oscillating plate is studied here by developing a model based on the Level

I GN equations. The right-hand side Cartesian coordinate system is used in the two dimensions, where x_1 points towards the wave propagation direction and x_2 points up, against the gravity. The fluid domain is bounded by top and bottom deformable curves, and is assumed to be incompressible and inviscid.

The GN equations satisfy the nonlinear boundary conditions and conservation of mass exactly, and postulate the conservation of momentum in an integrated form. There is no limitation for the irrotationality of the flow, i.e., the fluid flow can be rotational, see [20]. The only assumption made about the fluid kinematics in the GN equations is the distribution of the vertical velocity over the fluid column, which determines the levels of the GN equations, see [21]. In the Level I GN model, the vertical velocity varies linearly within the water column and thus the horizontal velocity is invariant in vertical direction. The Level I GN model is best applied for propagation of long waves in shallow water, see e.g. [4], [19] and [22]. For higher level GN equations, the vertical velocity field is prescribed as high-order polynomials, see e.g. [23], [24] and [25]. See [26] for wave refraction and diffraction by the Level I GN equations.

The Level I GN equations, used in this study, give the conservations of mass and momentum as (see [27])

$$\eta_{,t} + \{(h+\eta-\alpha)u_1\}_{,x_1} = \alpha_{,t}\,, \tag{1}$$

$$\begin{aligned} &\dot{u}_1 + g\eta_{,x_1} + \frac{\hat{p}_{,x_1}}{\rho} = -\frac{1}{6}\{[2\eta+\alpha]_{,x_1}\ddot{\alpha} \\ &+ [4\eta-\alpha]_{,x_1}\ddot{\eta} + (h+\eta-\alpha)[\ddot{\alpha}+2\ddot{\eta}]_{,x_1}\}\,, \end{aligned} \tag{2}$$

where u_1 and u_2 are fluid particle velocities in the x_1 and x_2 directions, respectively, $\hat{p}$ is the pressure on the top curve of the fluid domain, α is the deformation of the bottom curve, η is the surface elevation, ρ is the fluid density and g is the gravity acceleration. Subscripts after comma indicate differentiation with respect to the corresponding variables. $\dot{\theta}$ and $\ddot{\theta}$ are the first and second total derivatives of the arbitrary variable $\theta(x_1,t)$, respectively.

Following the approach proposed by [28] for wave propagation over a fixed, horizontal plate, shown in Fig. 1 in studying the wave interaction with a submerged oscillating plate, the fluid domain is divided into four regions: (i) RI, $x_1 < X_L$, the upwave region from the leading edge of the plate, (ii) RII, $X_L \le x_1 \le X_T$, the region above the oscillating plate, (iii) RIII, $X_L \le x_1 \le X_T$, the region below the plate, and (iv) RIV, $x_1 > X_T$, the downwave region from the trailing edge of the plate. Appropriate equations and boundary conditions are then applied to each region.

In Regions RI and RIV, the seafloor is flat and stationary, i.e. $\alpha(x_1,t) = 0$. The top boundary of the domain is free, i.e. $\eta = \eta(x_1,t)$, and it is exposed to the atmosphere, i.e. the top pressure is equal to the atmospheric pressure, taken as $\hat{p}(x_1,t) = 0$. Substituting $\alpha = \alpha_{,t} = \alpha_{,x_1} = 0$, $\hat{p} = 0$ and the constant water depth, $h = h_I$, into Eqs. (1) and (2), the resulting equations for regions RI and RIV are given as

$$\eta_{,t} + \{(h_I+\eta-\alpha)u_1\}_{,x_1} = 0\,, \tag{3}$$

$$\dot{u}_1 + g\eta_{,x_1} = -\frac{1}{3}\{2\eta_{,x_1}\ddot{\eta} + (h_I+\eta)\ddot{\eta}_{,x_1}\}\,. \tag{4}$$

The unknowns in RI and RIV are the free surface elevation, η, and the horizontal velocity, u_1.

In Region RII, $\eta = \eta(x_1,t)$, and $\hat{p}(x_1,t) = 0$, similar to that in Regions RI and RIV. The bottom curve of Region RII is the oscillating plate. In this study, we assume that the plate is flat and rigid and its oscillations are only allowed in the vertical direction and the water depth in RII is fixed at $h = h_{II} = \zeta_0$. Therefore, the vertical elevation of the plate in RII is taken as $\alpha(x_1,t) = \alpha(t)$. Substituting these conditions into Eqs. (1) and (2) gives the governing equations of wave propagation over a vertically oscillating floor as

$$\eta_{,t} + [(\zeta_0+\eta-\alpha)u_1]_{,x_1} = \alpha_{,t}\,, \tag{5}$$

$$\dot{u}_1 + g\eta_{,x_1} = -\frac{1}{3}\{(\ddot{\alpha}+2\ddot{\eta})\eta_{,x_1} + (\zeta_0+\eta-\alpha)\ddot{\eta}_{,x_1}\}\,. \tag{6}$$

The unknowns in Region RII are η, u_1 and α.

Region RIII consists of a horizontal, oscillating plate on its top, and a flat, stationary seafloor in the bottom, i.e. $\eta(x_1,t) = \eta(t)$ and $\alpha(x_1,t) = 0$ in RIII. The plate is assumed to be thin and thus the water depth in this region is $h = h_{III} = h_I - \zeta_0$. Substituting these conditions into Eqs. (1) and (2) gives

$$\eta_{,t} + (h_I-\zeta_0+\eta)u_{1,x_1} = 0\,, \tag{7}$$

$$\dot{u}_1 + \frac{\hat{p}_{,x_1}}{\rho} = 0\,, \tag{8}$$

where the unknowns in this region are η, u_1, and $\hat{p}$. Similar to RII, the number of equations (2) in RIII is one less than the number of unknowns (3) in RIII. Thus one more equation is required for Regions RII and RIII.

We assume that the fluid attaches to the plate without any gaps at all times, i.e., $\eta_{III}(t) = \alpha_{II}(t) = \zeta(t)$, where subscripts II and III refer to the variables of the regions. As shown in Fig. 1, ζ is measured from the plate's initial submergence depth, ζ_0. This relation closes the system of equations in RIII.

In RIII, substituting $\eta(x_1,t) = \zeta(t)$ into Eq. (7) gives

$$C_1(t) = -\frac{\zeta_{,t}}{h_I - \zeta_0 + \zeta}, \tag{9}$$

where C_1 is the integration constant and is only a function of time and is independent of x_1. Hence

$$u_1 = C_1 x_1 + C_2(t), \tag{10}$$

where C_2 is an integration constant, similar to C_1. Equation (10) illustrates that the horizontal velocity, in RIII, varies linearly in the x_1 direction, between the two ends of the plate.

The momentum equation in RIII, Eq. (8), can be expanded as

$$u_{1,t} + u_1 u_{1,x_1} + \frac{\hat{p}_{,x_1}}{\rho} = 0. \tag{11}$$

Substituting Eq. (10) into Eq. (11) gives

$$\hat{p} = -\frac{\rho}{2}\left(C_1^2 + C_{1,t}\right)x_1^2 - C_3(t), \tag{12}$$

where $C_3 = C_3(t)$ is the integration constant. That is, the top pressure in RIII, is distributed in a parabolic form between the leading and trailing edges of the plate.

Appropriate jump and matching conditions must be enforced at the leading and trailing edges of the plate to satisfy physics of the problem, and the continuity of mass and momentum across the discrete curves, see [29]. See [19] for more details about the jump and matching conditions, used in this study.

In the problem of wave interaction with a submerged oscillating plate, we assume that the plate is rigid and flat. The vertical motion of the plate is controlled by a linear spring and damper. Wave-induced oscillations of the plate are therefore given by Newton's second law as

$$\Sigma F = m\zeta_{,tt}, \tag{13}$$

where m is the mass of the plate, and $\Sigma F = F_{x_2} + F_f + F_k + F_{PT}$ is the sum of external loads on the plate, including: (i) the vertical wave loads, $F_{x_2}(t)$, (ii) the friction force between the plate and the rod, $F_f(t) = -\left(\frac{|\zeta_{,t}|}{\zeta_{,t}}\right)\mu F_{x_1}$, where $F_{x_1}(t)$ is the horizontal wave force on the plate, (iii) the spring force, $F_k(t) = -k(\zeta - \zeta_0)$, where k is the spring constant stiffness, and (iv) the damping force, $F_{PT}(t) = -C_d\zeta_{,t}$, where C_d is the damping coefficient. The plate is initially located at the equilibrium position ($x_2 = -\zeta_0$) where the weight of the plate, buoyancy and the spring forces are balanced.

The entire system of equations are discretized by use of the finite-difference method. The fluid domain is discretized into a set of mesh points and all continuous variables are approximated by the discrete values at the mesh nodes. Spatial derivatives are approximated by use of the second-order central difference method. The second-order modified Euler method is applied for time-marching, and the Gaussian Elimination method is used to solve the systems of equations. See [19] and [30] for more details on the numerical solutions used for this model.

The schematic of the numerical wave tank of wave interaction with a submerged, oscillating horizontal plate is shown in Fig. 1. A wave maker and a wave absorber are used on the left and right boundaries of the domain, respectively. The origin of the coordinate system is located on the still-water level (SWL). Water surface elevation η is measured form the SWL.

WAVE REFLECTION AND TRANSMISSION COEFFICIENTS

In this study, wave attenuation by oscillating plates is determined by the wave reflection and transmission coefficients. To calculate the reflection and transmission coefficients, the four-gauge method of [31] is applied. In this approach gauges GI and GII, are placed upwave from the leading edge of the plate, and gauges GIII and GIV, are placed downwave from the trailing edge of the plate, shown in Fig. 1. This method has been used successfully by [4] and [32] for problems involving nonlinear wave interaction with structures by the Level I GN equations.

In this approach, water surface elevation at a given location (gauge) is split into a series of linear waves of different amplitude, frequency and phase by use of the Fourier Transform method. The reflected and transmitted wave amplitudes of the n^{th} order harmonic, $A_R^{(n)}$ and $A_T^{(n)}$, are decomposed from the surface elevations upwave and downwave, respectively. Hence, to better assess the nonlinear

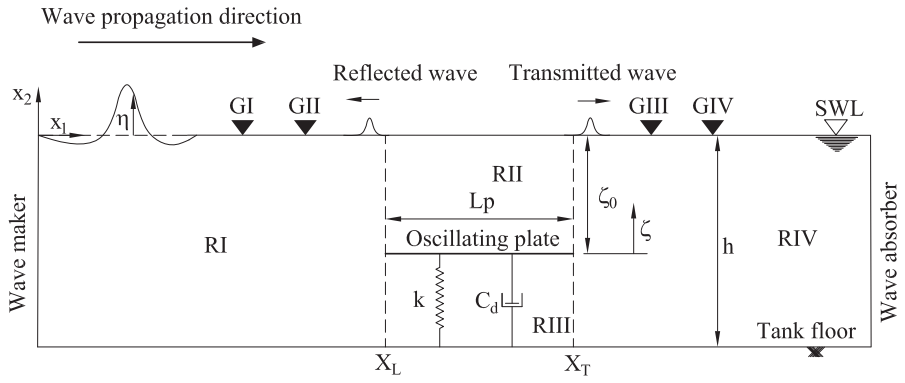

FIGURE 1. Schematic of the numerical wave tank of wave interaction with a fully submerged horizontal oscillating plate. The length of the plate is L_P and the plate is connected to a spring and a damper, whose spring stiffness is k and damping coefficient is C_d, respectively. ζ is the instantaneous position of the plate, measured from its initial submergence depth, ζ_0.

effects, the first three harmonic amplitudes ($n = 1,2$ and 3) are used to calculate wave reflection and transmission coefficients. Wave reflection and transmission coefficients, $C_R^{(n)}$, and $C_T^{(n)}$, are given as

$$C_R^{(n)} = \frac{A_R^{(n)}}{A_I}, \quad C_T^{(n)} = \frac{A_T^{(n)}}{A_I}, \tag{14}$$

where A_I is the incident wave amplitude.

COMPARISON OF SURFACE ELEVATION TIME SERIES

In this paper, all variables are dimensionless by use of ρ, g and h, such that

$$\begin{aligned} &x_1' = \frac{x_1}{h}, \quad \eta' = \frac{\eta}{h}, \quad \lambda' = \frac{\lambda}{h}, \quad H' = \frac{H}{h}, \\ &L_p' = \frac{L_p}{h}, \quad \zeta_0' = \frac{\zeta_0}{h}, \quad t' = t\sqrt{\frac{g}{h}}, \\ &m' = \frac{m}{\rho h^2 B}, \quad k' = \frac{k}{\rho g h B}, \quad C_d' = \frac{C_d}{\rho\sqrt{gh}Bh}, \end{aligned} \tag{15}$$

where λ is wavelength, H is wave height, and B is the plate width (into the page). Superscript ($\prime$) is removed from all variables for simplicity in the following sections.

In this section, we compare time series of surface elevation by the GN model with the available data, including laboratory experiments, and the NS and linear models of [19]. Figure 2 shows time series of surface elevation, obtained by the GN, and the available data of laboratory measurements, and the NS and linear models, recorded at $x_1 = X_L - 2$ upwave from the leading edge of the plate, and $x_1 = X_T + 2$ downwave from the trailing edge, for two wave heights, $H = 0.067$ and $H = 0.133$. The length and mass of the plate are $L_P = 1$ and $m = 0.016$, respectively. See [19] for more details about the laboratory experiments. The GN results show very good agreement with the laboratory experiments The NS and linear approaches predict slightly smaller upwave amplitude than that of the GN model. The GN and NS models show closer agreement downwave of the plate.

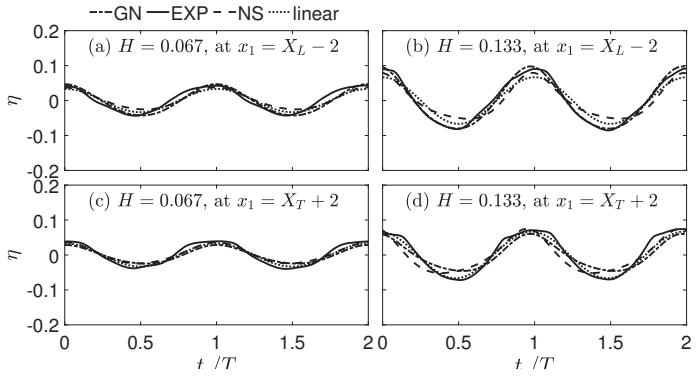

FIGURE 2. Comparison of time series of surface elevation, recorded upwave (a, b) and downwave (c, d), for $H = 0.067$ and $H = 0.133$ by the GN and laboratory experiments, and NS and linear models. $T = 10$, $\zeta_0 = 0.3$, and $k = 0.041$.

Next, time series of the surface elevation, calculated by the GN is compared with the NS model of [19], shown in Fig. 3 for $\zeta_0 = 0.4$, and $k = 3$, Fig. 4 for $\zeta_0 = 0.6$, and $k = 3$, and Fig. 5 for $\zeta_0 = 0.4$, and $k = 15$. The length and mass of the plate are $L_P = 3$ and $m = 0.35$, respectively. The locations of gauges upwave for GI and GII and downwave

for GIII and GIV are fixed at $x_1 = X_L - 6$ and $x_1 = X_L - 3$, and $x_1 = X_T + 3$ and $x_1 = X_T + 6$, respectively.

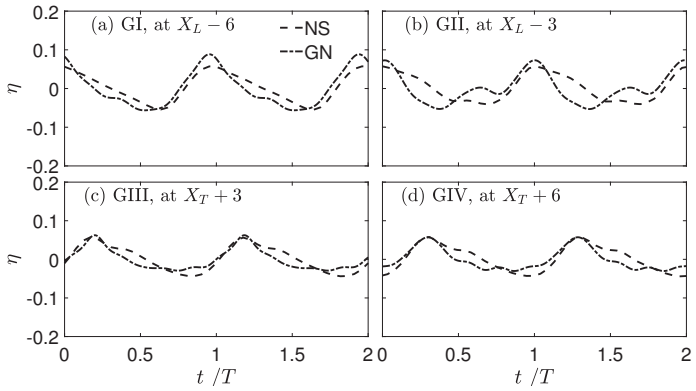

FIGURE 3. Comparisons of time series of surface elevation by the NS and GN models for $\zeta_0 = 0.4$ and $k = 3$. $T = 25$, $H = 0.1$.

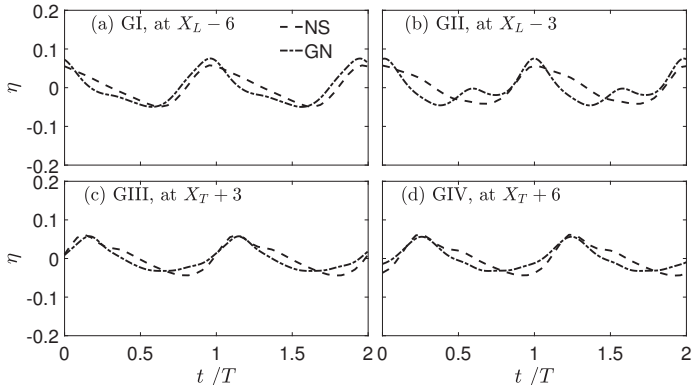

FIGURE 4. Comparisons of time series of surface elevation by the NS and GN models for $\zeta_0 = 0.6$ and $k = 3$. $T = 25$, $H = 0.1$.

Shown in Figs. 3, 4 and 5, the GN model predicts the peak of the surface elevation slightly larger in GI, upwave from the leading edge. In all other gauges, results of the GN model are in close agreement with the NS model particularly at the downwave gauges.

RESULTS AND DISCUSSIONS

In this section, wave reflection and transmission coefficients are calculated and their nonlinear components up to the third-order harmonics are considered. Results are obtained by use of the GN model, and presented and discussed for a range of variables. Wave gauges GI, GII, GIII and GIV, used in this section, are placed upwave and downwave as shown in Fig. 1, and their locations are determined depending on the wavelength (λ) and given in Table 1.

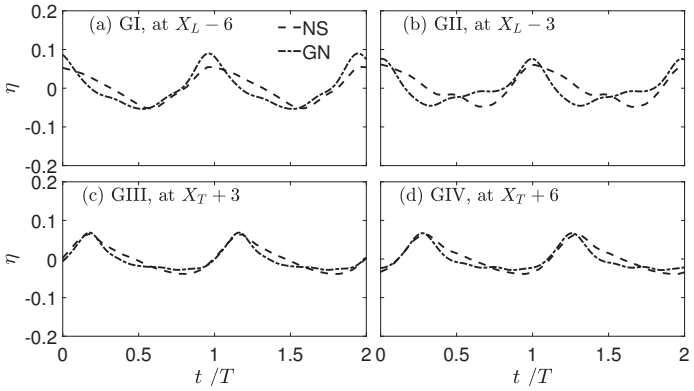

FIGURE 5. Comparisons of time series of surface elevation by the NS and GN models for $\zeta_0 = 0.4$ and $k = 15$. $T = 25$, $H = 0.1$.

TABLE 1. Wave gauge locations with variation of wavelength.

λ	GI	GII	GIII	GIV
6	$X_L - 10$	$X_L - 7.7$	$X_T + 7.7$	$X_T + 10$
8	$X_L - 10$	$X_L - 7.7$	$X_T + 7.7$	$X_T + 10$
10	$X_L - 10$	$X_L - 7.7$	$X_T + 7.7$	$X_T + 10$
12	$X_L - 10$	$X_L - 7.7$	$X_T + 7.7$	$X_T + 10$
16	$X_L - 10$	$X_L - 5.4$	$X_T + 5.4$	$X_T + 10$
20	$X_L - 10$	$X_L - 5.4$	$X_T + 5.4$	$X_T + 10$
24	$X_L - 10$	$X_L - 5.4$	$X_T + 5.4$	$X_T + 10$

A wide range of parameters, including wavelength λ, wave height, plate length, initial submergence depth of the plate, spring stiffness and damping coefficients, are considered to investigate their effect on the wave attenuation, presented by $C_R^{(n)}$ and $C_T^{(n)}$. Values of these variables are given in Table 2. The oscillating plate is not changed and $L_P = 2$ and $m = 0.2$ are constant and $C_d = 0.0$, in this section, unless otherwise stated.

EFFECT OF WAVELENGTH

Figure 6 shows the variation of $C_R^{(n)}$ and $C_T^{(n)}$ with λ/L_P for different initial submergence depths, $\zeta_0 = 0.2$, 0.4 and 0.6. Shown in Fig. 6, $C_R^{(n)}$ and $C_T^{(n)}$vary nonlinearly with λ/L_P. The nonlinear components, $C_R^{(2)}$ and $C_T^{(2)}$, and $C_R^{(3)}$

TABLE 2. Values of variables considered in this study.

Variables	Values
λ	6, 8, 10, 12, 16, 20, 24
H	0.1, 0.15, 0.2, 0.25, 0.3, 0.35, 0.4
L_P	1, 2, 3, 4
ζ_0	0.2, 0.3, 0.4, 0.5, 0.6
k	0.3, 0.6, 1, 2, 3, 4, 6, 8, 10
C_d	0.0, 1.0, 5.0

and $C_T^{(3)}$, play more remarkable roles for longer waves, at $\lambda/L_P \geq 5$, in most cases.

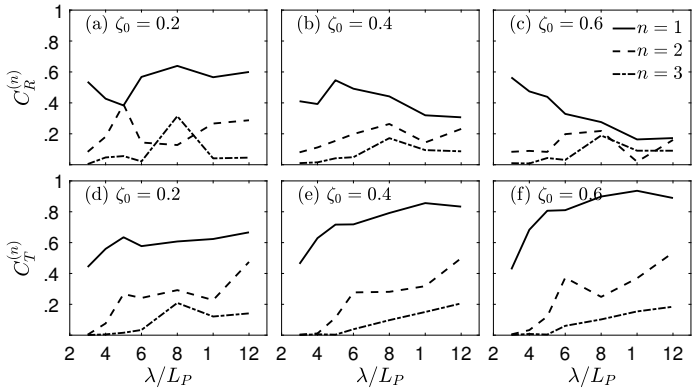

FIGURE 6. Variation of (a)-(c) wave reflection and (d)-(f) transmission coefficients with λ/L_P for $\zeta_0 = 0.2$, 0.4 and 0.6, and $H = 0.2$ and $k = 3$ are constant.

Shown in Fig. 6, the smallest $C_R^{(1)}$ value is observed at the largest wavelength ($\lambda/L_P = 12$), for larger initial submergence depths ($\zeta_0 = 0.4$ and 0.6). Peaks of $C_R^{(2)}$ and $C_R^{(3)}$ occur at $\lambda/L_P = 8$ for $\zeta_0 = 0.4$ and 0.6. The peak values of $C_R^{(2)}$ and $C_R^{(3)}$ at $\zeta_0 = 0.2$ are larger than that at $\zeta_0 = 0.4$ and 0.6, which shows that nonlinear components behave more significantly when the plate oscillates closer to the free surface, and this is of course not surprising. $C_T^{(1)}$ is nearly constant with increasing λ/L_P, while $C_T^{(2)}$ and $C_T^{(3)}$ are increasing in most cases.

EFFECT OF WAVE HEIGHT

Figure 7 shows variation of $C_R^{(n)}$ and $C_T^{(n)}$ with various wave heights for $C_d = 0.0$, 1.0 and 5.0. Shown in Fig. 7, $C_R^{(n)}$ and $C_T^{(n)}$ vary nonlinearly with wave height. Also, the damping coefficients hardly affect the wave reflection and transmission coefficients.

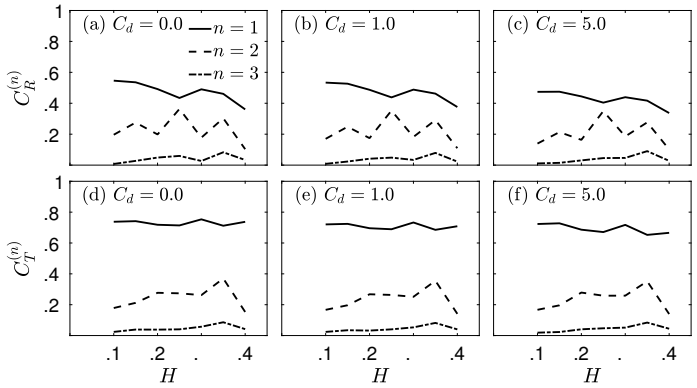

FIGURE 7. Variation of (a)-(c) wave reflection and (d)-(f) transmission coefficients with wave height H for $C_d = 0.0$, 1.0 and 5.0, and $\lambda = 12$, $\zeta_0 = 0.4$ and $k = 3$ are constant.

Shown in Fig. 7, $C_R^{(1)}$ and $C_R^{(2)}$ are smallest at $H = 0.4$ for all cases. $C_R^{(1)}$ generally decreases with increasing wave height while $C_R^{(2)}$ is oscillatory from $H = 0.1$ to $H = 0.4$, and its maximum value occur at an intermediate wave height, $H = 0.25$. The third-order components, $C_R^{(3)}$ and $C_T^{(3)}$, are not remarkable for all wave heights. Values of $C_T^{(1)}$ show less variation with wave height (H), roughly equals to 0.7 in nearly all cases. $C_T^{(2)}$ reaches a maximum value at a relatively larger wave height, $H = 0.35$, but it becomes much smaller with an increase in wave height.

EFFECT OF PLATE LENGTH

Figure 8 shows the variation of $C_R^{(n)}$ and $C_T^{(n)}$ with various plate lengths for $\lambda = 6$, $\lambda = 12$ and $\lambda = 24$. The length of the plate, as considered here, is between $Lp = 1$ and $Lp = 4$, with an interval of 1. The plate density is invariant and thus its corresponding mass is between $m = 0.1$ and $m = 0.4$, with an interval of 0.1.

As shown in Fig. 8, we find that wave attenuation behaves nonlinearly with plate length. The second-order and third-order harmonics rarely contribute to wave reflection and transmission for $\lambda = 6$. In this figure, $C_R^{(1)}$ is reversely changed with plate length for $\lambda = 6$ while $C_R^{(1)}$ is almost positively proportional with L_P for $\lambda = 12$ and $\lambda = 24$. This is mainly because the bottom pressure of the oscillating plate are distributed in a parabolic form. Wave forces acting on the plate vary nonlinearly with increasing plate lengths and thus plate oscillations are not identical even for

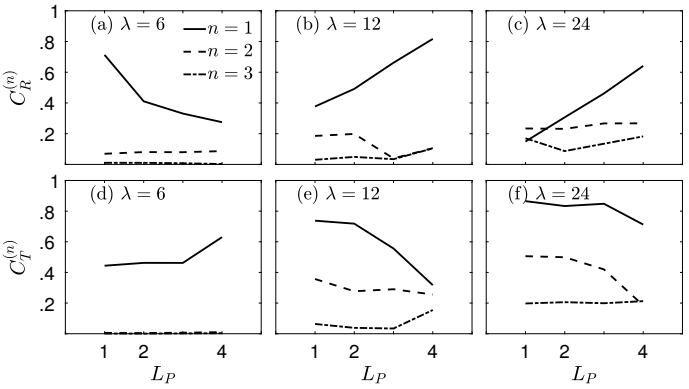

FIGURE 8. Variation of (a)-(c) wave reflection and (d)-(f) transmission coefficients with plate length L_P for $\lambda = 6$, 12 and 24, and $H = 0.2$ and $\zeta_0 = 0.4$ are constant.

the same λ/L_P, but a different plate length. Note that plate lengths are nondimensionalized by the fixed water depth, h.

EFFECT OF SPRING STIFFNESS

Variation of $C_R^{(n)}$ and $C_T^{(n)}$ with various spring stiffness for $\lambda = 6$, $\lambda = 12$ and $\lambda = 24$ are shown in Fig. 9. Similar to that in Fig. 6, nonlinearity has more significant effect on longer waves for different spring stiffness. The oscillating plates with a weaker spring attached to, i.e. $k \leq 1$, allow larger oscillations, and this causes larger wave reflection. With an increase in spring stiffness, e.g. $k \geq 4$, the oscillating plate attenuates waves nearly the same i.e. the reflection and transmission coefficients are almost constant.

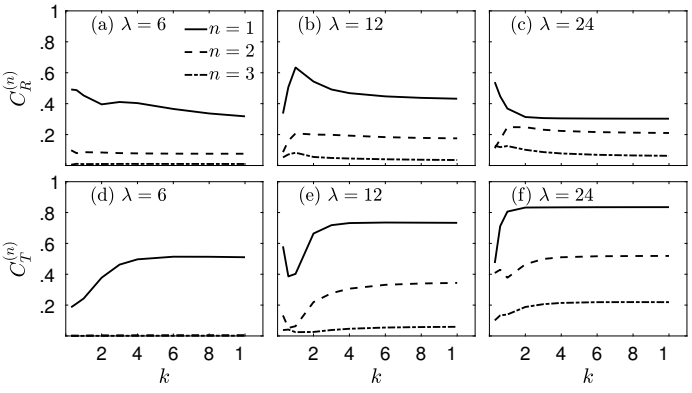

FIGURE 9. Variation of (a)-(c) wave reflection and (d)-(f) transmission coefficients with spring stiffness k for $\lambda = 6$, 12 and 24, and $H = 0.2$ and $\zeta_0 = 0.4$ are constant.

OSCILLATING VS FIXED SUBMERGED PLATE

In this section, we investigate differences in wave attenuation by a horizontal submerged oscillating plate and an equivalent horizontal submerged fixed plate. Identical wave-plate conditions are used for the fixed and oscillating submerged plates to allow for a direct comparison of the results. The only difference is that we use the model discussed here for the oscillating plate while the model of [22] is used for the fixed plate, which uses the Level I GN theory.

Figure 10 shows that surface elevation time series recorded in gauges GI and GII upwave and gauges GIII and GIV downwave of the oscillating plate are compared to that of the fixed plate. See [4] for a parametric study of

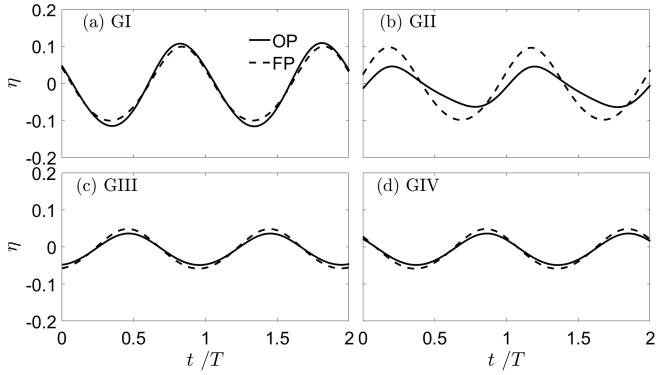

FIGURE 10. Comparisons of time series of surface elevation for (a, b) gauegs GI and GII upwave and (c, d) GIII and GIV downwave of the plate, attenuated by the oscillating plates (OP) and the fixed plates (FP). $\lambda = 6$, $H = 0.2$, $\zeta_0 = 0.5$, and $k = 3$.

wave interaction with a fixed, submerged horizontal plate. Shown in Fig. 10, wave amplitudes attenuated by the oscillating plate are slightly larger in gauge GI while the wave heights attenuated by the oscillating plate are smaller in other gauges, particularly in gauge GII.

Figure 11 illustrates variation of $C_R^{(n)}$ and $C_T^{(n)}$, of the oscillating plate and fixed plate with ζ_0 for three wavelengths $\lambda = 6$, 12 and 24. In Fig. 11, we can observe remarkable differences between the oscillating plate and fixed plate for shorter wavelength ($\lambda = 6$). However, $C_R^{(n)}$ and $C_T^{(n)}$, calculated by the oscillating plate, are much closer to the fixed plate for the longer wavelength ($\lambda = 24$). This is because pressure differences above and below the oscillating plate are not remarkable for long water waves, and thus the plate oscillations are limited, see [19].

CONCLUDING REMARKS

In this study, we developed a model based on the nonlinear Level I Green-Naghdi equations for the problem of wave propagation over the submerged oscillating plates. Attention is confined to wave attenuation by an oscillating

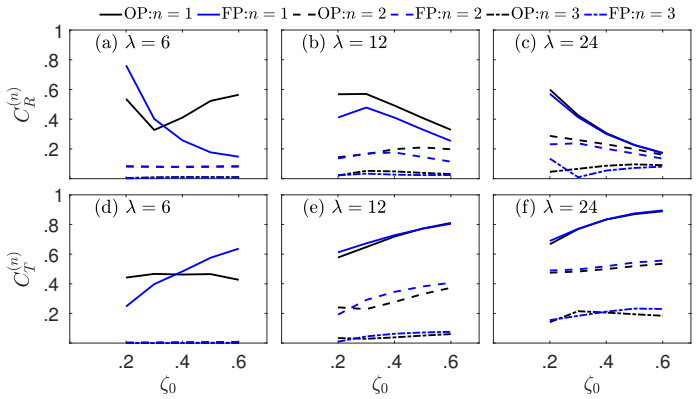

FIGURE 11. Variation of (a)-(c) wave reflection and (d)-(f) transmission coefficients of oscillating plates (OP) fixed plates (FP) with ζ_0 for $\lambda = 6$, 12 and 24, and $H = 0.2$ and $k = 3$ are constant.

plate in shallow water. Wave reflection and transmission coefficients, $C_R^{(n)}$ and $C_T^{(n)}$, are determined to evaluate the reflected and transmitted waves, respectively. To investigate the contributions of nonlinear components to attenuated waves, the first three harmonics are considered in this study.

Time series of surface elevation of the model are compared with the laboratory experiments, the NS and linear models of [19]. Good agreement is observed between the GN results and experimental data and the other two numerical results.

Variations of $C_R^{(n)}$ and $C_T^{(n)}$ with various parameters, including wavelength, wave height, plate length, initial submergence depth of the plate, spring stiffness and damping coefficients, are investigated as well in this study.

Overall nonlinear harmonics play an important role to determine wave attenuation by the oscillating plate in shallow water. $C_R^{(2)}$ and $C_T^{(2)}$, are remarkable in most cases while $C_R^{(3)}$ and $C_T^{(3)}$, are less significant in some cases.

In this study, a wide range of parameters are considered to investigate their effect on wave attenuation by a submerged oscillating plate. The relation of λ/L_P to $C_R^{(n)}$ and $C_T^{(n)}$ is nonlinear. Nonlinear harmonic components play more remarkable effect on the wave attenuation for longer waves. Initial submergence depth of the oscillating plate has more remarkable influence on the first harmonic, $C_R^{(1)}$ and $C_T^{(1)}$, than that of the higher-order components. The effect of wave height on $C_T^{(n)}$ is less than that on $C_R^{(n)}$. The damping coefficients show small effect on $C_R^{(n)}$ and $C_T^{(n)}$ for the cases considered in this study. Plate lengths nonlinearly affect the plate oscillations, and wave reflection and transmission coefficients are not identical for the same λ/L_P but a different plate length. Springs, attached to the plate, dominate the performance of wave attenuation where oscillations of the plate are hardly altered with relatively stronger springs, i.e., $C_R^{(n)}$ and $C_T^{(n)}$ are almost invariant in these cases.

Wave attenuation by an oscillating plate are calculated by use of the GN model, and compared with that of a fixed plate. We find that differences of wave attenuation by the oscillating and fixed plates are more remarkable for shorter waves.

Overall, it is observed that an oscillating submerged plate can have remarkable effect on the wave field. In almost all cases considered here, the presence of the oscillating plate increase the nonlinearity in the flow field.

REFERENCES

[1] Liu, P. L.-F., and Iskandarani, M., 1991. "Scattering of short-wave groups by submerged horizontal plate". *Journal of Waterway, Port, Coastal, and Ocean Engineering,* ***117***(3), pp. 235–246.

[2] Carter, R. W., Ertekin, R. C., and Lin, P., 2006. "On the reverse flow beneath a submerged plate due to wave action". In International Conference on Offshore Mechanics and Arctic Engineering, OMAE2006, June 4-9, Hamburg, Germany, pp. OMAE2006–92623.

[3] Brossard, J., Perret, G., Blonce, L., and Diedhiou, A., 2009. "Higher harmonics induced by a submerged horizontal plate and a submerged rectangular step in a wave flume". *Coastal Engineering,* ***56***(1), pp. 11–22.

[4] Hayatdavoodi, M., Ertekin, R. C., and Valentine, B. D., 2017. "Solitary and cnoidal wave scattering by a submerged horizontal plate in shallow water". *AIP Advances,* ***7***, pp. 065212–29.

[5] Huang, L., and Li, Y., 2022. "Design of the submerged horizontal plate breakwater using a fully coupled hydroelastic approach". *Computer-Aided Civil and Infrastructure Engineering,* ***37***(7), pp. 915–932.

[6] Zheng, S., Liang, H., Michele, S., and Greaves, D., 2023. "Water wave interaction with an array of submerged circular plates: Hankel transform approach". *Physical Review Fluids,* ***8***(1), p. 014803.

[7] Liu, C. R., Huang, Z. H., and Chen, W. P., 2017. "A numerical study of a submerged horizontal heaving plate as a breakwater". *Journal of Coastal Research,* ***33***(4), pp. 917–930.

[8] He, M., Xu, W., Gao, X., and Ren, B., 2018. "SPH simulation of wave scattering by a heaving submerged

horizontal plate". *International Journal of Ocean and Coastal Engineering,* ***1***(02), p. 1840004.

[9] Fu, D., Zhao, X. Z., Wang, S., and Yan, D. M., 2021. "Numerical study on the wave dissipating performance of a submerged heaving plate breakwater". *Ocean Engineering,* ***219***, p. 108310.

[10] Mendoza, E., Silva, R., Zanuttigh, B., Angelelli, E., Andersen, T. L., Martinelli, L., Nørgaard, J. Q. H., and Ruol, P., 2014. "Beach response to wave energy converter farms acting as coastal defence". *Coastal Engineering,* ***87***, pp. 97–111.

[11] Borgarino, B., Babarit, A., and Ferrant, P., 2012. "Impact of wave interactions effects on energy absorption in large arrays of wave energy converters". *Ocean Engineering,* ***41***, pp. 79–88.

[12] Carter, R. W., and Ertekin, R. C., 2014. "Focusing of wave-induced flow through a submerged disk with a tubular opening". *Applied Ocean Research,* ***47***, pp. 110–124.

[13] Newman, J. N., 2015. "Amplification of waves by submerged plates". In 30th international workshop on water waves and floating bodies (IWWWFB), Bristol, UK, pp. 153–156.

[14] Zheng, S., Meylan, M., Greaves, D., and Iglesias, G., 2020. "Water-wave interaction with submerged porous elastic disks". *Physics of Fluids,* ***32***(4), p. 047106.

[15] Liang, H., Zheng, S., Shao, Y., Chua, K. H., Choo, Y. S., and Greaves, D., 2021. "Water wave scattering by impermeable and perforated plates". *Physics of Fluids,* ***33***(7), p. 077111.

[16] Patarapanich, M., 1984. "Maximum and zero reflection from submerged plate". *Journal of Waterway, Port, Coastal, and Ocean Engineering,* ***110***(2), pp. 171–181.

[17] Dick, T. M., and Brebner, A., 1968. "Solid and permeable submerged breakwaters". *Coastal Engineering Proceedings,* ***1***(11), pp. 1141–1158.

[18] Hayatdavoodi, M., Wagner, J. J., Wagner, J. R., and Ertekin, R. C., 2016. "Vertical oscillation of a horizontal submerged plate". In 31st International Workshop on Water Waves and Floating Bodies (IWWWFB), April 3-6, Plymouth, Michigan, USA.

[19] Hayatdavoodi, M., Chen, Y. B., Zhao, B. B., and Ertekin, R. C., 2023. "Experiments and computations of wave-induced oscillations of submerged horizontal plates". *Physics of Fluids,* ***35***(1), pp. 017121(1–28).

[20] Green, A. E., and Naghdi, P. M., 1976. "Directed fluid sheets". *Proceedings of the Royal Society of London. A. Mathematical and Physical Sciences,* ***347***(1651), pp. 447–473.

[21] Green, A. E., and Naghdi, P. M., 1976. "A derivation of equations for wave propagation in water of variable depth". *Journal of Fluid Mechanics,* ***78***(2), pp. 237–246.

[22] Hayatdavoodi, M., and Ertekin, R. C., 2015. "Wave forces on a submerged horizontal plate – part I: Theory and modelling". *Journal of Fluids and Structures,* ***54***, pp. 566–579.

[23] Webster, W. C., Duan, W. Y., and Zhao, B. B., 2011. "Green-Naghdi theory, Part A: Green-Naghdi (GN) equations for shallow water waves". *Journal of Marine Science and Application,* ***10***(3), pp. 253–258.

[24] Zhao, B. B., Duan, W. Y., and Ertekin, R. C., 2014. "Application of higher-level GN theory to some wave transformation problems". *Coastal Engineering,* ***83***, pp. 177–189.

[25] Zhao, B. B., Duan, W. Y., Ertekin, R. C., and Hayatdavoodi, M., 2015. "High-level Green-Naghdi wave models for nonlinear wave transformation in three dimensions". *Journal of Ocean Engineering and Marine Energy,* ***1***(2), pp. 121–132.

[26] Hayatdavoodi, M., and Ertekin, R. C., 2022. "Diffraction and refraction of nonlinear waves by the Green–Naghdi equations". *Journal of Offshore Mechanics and Arctic Engineering,* ***145***(2), p. 021201.

[27] Ertekin, R. C., 1984. *Soliton Generation by Moving Disturbances in Shallow Water: Theory, Computation and Experiment*. Ph.D. Dissertation, University of California, Berkeley.

[28] Hayatdavoodi, M., and Ertekin, R. C., 2015. "Nonlinear Wave Loads on a Submerged Deck by the Green-Naghdi Equations". *Journal of Offshore Mechanics and Arctic Engineering,* ***137***(1), p. 11102.

[29] Naghdi, P. M., and Rubin, M. B., 1981. "On the transition to planing of a boat". *Journal of Fluid Mechanics,* ***103***, pp. 345–374.

[30] Hayatdavoodi, M., and Ertekin, R. C., 2015. "Wave forces on a submerged horizontal plate – part II: Solitary and cnoidal waves". *Journal of Fluids and Structures,* ***54***, pp. 580–596.

[31] Grue, J., 1992. "Nonlinear water waves at a submerged obstacle or bottom topography". *Journal of Fluid Mechanics,* ***244***, pp. 455–476.

[32] Kostikov, V., Hayatdavoodi, M., and Ertekin, R. C., 2021. "Hydroelastic interaction of nonlinear waves with floating sheets". *Theoretical and Computational Fluid Dynamics,* ***35***, pp. 515–537.